

A way to synchronize models with seismic faults for earthquake forecasting: Insights from a simple stochastic model

Álvaro González^{a,1} Miguel Vázquez-Prada^b Javier B. Gómez^a
Amalio F. Pacheco^b

^a*Departamento de Ciencias de la Tierra. Universidad de Zaragoza.
C./ Pedro Cerbuna, 12. 50009 Zaragoza, Spain.*

^b*Departamento de Física Teórica and BIFI. Universidad de Zaragoza.
C./ Pedro Cerbuna, 12. 50009 Zaragoza, Spain.*

Abstract

Numerical models of seismic faults are starting to be used for determining the future behaviour of seismic faults and fault networks. Their final goal would be to forecast future large earthquakes. In order to use them for this task, it is necessary to synchronize each model with the current status of the actual fault or fault network it simulates (just as, for example, meteorologists synchronize their models with the atmosphere by incorporating current atmospheric data in them). However, lithospheric dynamics is largely unobservable: important parameters cannot (or can rarely) be measured in Nature. Earthquakes, though, provide indirect but measurable clues of the stress and strain status in the lithosphere, which should be helpful for the accurate synchronization of the models.

The rupture area is one of the measurable parameters of actual earthquakes. Here we explore how this can be used to at least synchronize fault models between themselves and forecast synthetic earthquakes. Our purpose here is to forecast synthetic earthquakes in a simple but stochastic (random) fault model. By imposing the rupture area of the synthetic earthquakes of this model on other models, the latter become partially synchronized with the first one. We use these partially synchronized models to successfully forecast most of the largest earthquakes generated by the first model. This forecasting strategy outperforms others that only take into account the earthquake series. Our results suggest that probably a good way to synchronize more detailed models with real faults is to force them to reproduce the sequence of previous earthquake ruptures on the faults. This hypothesis could be tested in the future with more detailed models and actual seismic data.

Key words: Characteristic earthquakes, earthquake prediction, fault model, seismic modelling, seismic quiescence, synthetic-earthquake catalogues.

1 Introduction: Data assimilation in dynamical fault models

Numerical models are now frequently used to simulate the seismic behaviour of real faults (e.g. Kato and Seno, 2003; Fitzenz and Miller, 2004; Kuroki et al., 2004) and fault networks (e.g. Ward, 2000; Hashimoto, 2001; Robinson and Benites, 2001; Rundle et al., 2001; Soloviev and Ismail-Zadeh, 2003; Robinson, 2004; Rundle et al., 2004). In these models, fault planes separate lithospheric blocks that are strained at specific rates, and sudden slips (earthquakes) are generated by the faults according to certain friction and/or rupture laws. Although no completely realistic dynamical model presently exists, these simulations are now sufficiently credible to begin to play a substantial role in scientific studies of earthquake probability and hazard (Ward, 2000). The final goals of the numerical modelling of seismicity are not different from, for example, the goals of numerical models of the atmosphere. A good model should be able to

- (1) reproduce the general characteristics of the system,
- (2) mimic the state of the system at the present moment, and
- (3) forecast the future evolution of the system.

Most numerical models of seismicity have been designed to achieve the first goal, by reproducing general characteristics of earthquakes such as their size-frequency distribution (e.g. Bak and Tang, 1989; Olami et al., 1992; Dahmen et al., 1998; Preston et al., 2000; Vázquez-Prada et al., 2002), or the generation of aftershock and foreshocks (e.g. Hainzl et al., 1999). When a model is designed this way, it is left to evolve freely according to its rules, and all that is checked is whether the overall results of the model are similar to the observations made in Nature or not.

When dealing with the second goal, new issues arise. It requires data assimilation, that is, the process of absorbing and incorporating observed information into the model. By this process, the model is tuned and synchronized, at least partially, with the real system it tries to simulate. In a meteorological model, data of atmospheric pressure, temperature, humidity, cloud cover, precipitation, etc. measured in a given moment at different locations and heights can be included. With this procedure, the model becomes a reasonably good representation of the atmosphere at that moment. Then it can be used to calculate the probable future atmospheric evolution (i.e. the third goal cited above).

Seismic data assimilation poses greater problems than its meteorological equivalent. This explains (at least partially) the relative delay in developing reliable forecasts of large earthquakes. The inner workings of both the atmosphere (Houghton, 2002) and the lithosphere (Goltz, 1997; Turcotte, 1997;

¹ Corresponding author.

E-mail: Alvaro.Gonzalez@unizar.es

Keilis-Borok, 2002) are complex and chaotic, so they are inherently difficult to forecast. However, while Meteorologists can probe the atmosphere every day at different places and heights (and assimilate the obtained data in their models in near real-time), lithospheric variables of paramount importance, such as the stress and strain, can be measured only in certain places, and not at any time: earthquakes have unobservable dynamics (Rundle et al., 2003). For example, the best current compendium of stress magnitudes and directions in the lithosphere is the World Stress Map (Zoback, 1992; Reinecker et al., 2004), whose entries are point static time-averaged estimates of maximum and minimum principal stresses in space. And the direct measurements of stress on active fault zones at depth are still scarce (e.g. Ikeda et al., 2001; Tsukahara et al., 2001; Yamamoto and Yabe, 2001; Hickman and Zoback, 2004; Boness and Zoback, 2004). The dynamical models would need better spatial and temporal information of stress, both more abundant and more systematically collected than that currently available (Rundle et al., 2004). It is thus necessary to seek ways to tune and synchronize the models with more abundant observable data.

A first step of data assimilation in models of earthquake faults is to introduce information regarding the topology (that is, the shape and location) of the active faults and their long-term behaviour. For example, the long-term fault slip rate, and the average recurrence interval of the largest earthquakes in the fault can be estimated from paleoseismological studies and should be included in the models (Grant and Gould, 2004). Examples of this approach are the works of Rundle et al. (2001, 2004) and Robinson (2004). The surface deformation measured via Global Positioning System (GPS) networks and by Synthetic Aperture Radar Interferometry (InSAR) can also constitute input data for the dynamical fault models (Rundle et al., 2004). Earthquakes themselves are indeed the most obvious observable events of lithospheric dynamics, and could provide the most detailed data available to assimilate in the models, but how? The earthquake rupture area could be an important clue.

The rupture area and slip distribution in real earthquakes can be very complex (Sieh, 1996; Kanamori and Brodsky, 2004), but can be estimated in a variety of ways. The actual slip distribution can be obtained by inverting the observed seismic waveforms (Kanamori and Brodsky, 2004) and/or by geodetic modelling of surface displacement (Yabuki and Matsuura, 1992). Some earthquakes produce surface ruptures, which are useful for estimating the rupture area (Stirling et al., 2002). Although most surface ruptures occur in large shocks, with magnitudes larger than 6, they have been reported for earthquakes with magnitudes M_L down to 2.5 (see the extensive compilation of historic earthquakes with surface rupture by Yeats et al., 1997, pp. 473-485). Also, the rupture area can be estimated from the seismic moment, (which is calculated from seismic, geodetic or geological data; Kanamori and Brodsky, 2004) or from the moment magnitude (Wells and Coppersmith, 1994; Stirling et al., 2002; Dowrick and Rhoades, 2004). Frequently the location of early after-

shocks is used to determine the rupture area of the mainshock (Wells and Coppersmith, 1994), although the aftershock zone tends to grow with time (Kisslinger, 1996) and is not necessarily a good indicator of that area (Yagi et al., 1999).

Complex models with realistic fault topology are able to reproduce the rupture area and coseismic slip of historical earthquakes. It is thus possible to force the model to reproduce the rupture of a historical earthquake, and let it evolve from that moment onwards to see what could happen in the future. For example, Ward (2000) developed a model including the network of main faults in the San Francisco Bay Area (California). He forced the model to reproduce the San Andreas Fault surface coseismic slip of the 1906 San Francisco earthquake, and let it evolve freely from that earthquake onwards, in an attempt to simulate the probable sequence of earthquake ruptures during the next 3000 years.

But considering only the data of the largest earthquake in the series is probably not sufficient to properly synchronize the model. Complex and chaotic systems are very sensitive to the initial conditions. The information regarding only one event probably does not sufficiently constrain the initial conditions, and the calculated evolution will probably be a particular case of a large range of possible outcomes. Will this panorama improve by forcing the model to reproduce all the observed earthquake ruptures, including the small ones? Probably yes. To check whether this idea works, at least with a simple model, is the purpose of this paper.

In the following sections, our goal will be to forecast the largest earthquakes generated by the minimalist model, a simple numerical fault model. We will show that when all the earthquake ruptures generated by this model are imposed on other, similar models, these become partially synchronized with the former. We use them to declare alarms that efficiently mark the occurrence of the largest shocks in the first model. The results are much better than those obtained with other strategies that consider only the earthquake series. The model, albeit simplistic, is stochastic (it involves randomness), so its efficient forecasting is not trivial. We will describe how this stochasticity can be dealt with, by using an approach similar to the so-called ensemble forecasting used in Meteorology (Palmer et al., 2005). The method could be used in other more detailed and realistic models (stochastic or not) to test our general conclusion: that they might be partially synchronized with actual faults by being forced to reproduce the series of observed earthquake ruptures.

In the next section we describe the model and its properties. Then, we outline the general scheme of prediction and the forecasting strategies used as reference to assess the merits of any other predictive method in the model. Finally, the method based on partial synchronization is explained and its possible utility discussed.

2 The minimalist model

In this section we will describe the minimalist model, the numerical model whose largest synthetic earthquakes we will try to forecast. We introduced this model in a previous paper (Vázquez-Prada et al., 2002). The minimalist model has mainly two, apparently contradictory, advantages for the purpose of this paper: it is simple but, at the same time, it is difficult to forecast. Because it is simple, several of its properties can be derived analytically, and it can be characterized in detail with numerical simulations which do not require an impractical amount of computer time. Because it is stochastic, it is difficult to forecast, so the results we will obtain here are not trivial. In the following paragraphs we will explain how the model works, and what are its main properties, comparing them with those of actual faults.

2.1 *How the model works*

The model is a simple (hence its name) cellular automaton. Cellular automata are frequently used to model seismic faults. In these models, the fault plane is divided into a grid of cells, and the time evolves in discrete time steps. Each cell's state is updated at each time step according to rules that usually depend on the state of the cell or that of its neighbors in the previous time step. These rules can be designed according to certain friction laws (Ben-Zion, 2001), stress transfer (Olami et al., 1992; Hainzl et al., 1999; Preston et al., 2000), and the effect of fluids (Miller et al., 1999). In the minimalist model, as well as in other very simple cellular automata (e.g. Newman and Turcotte, 2002; González et al., 2005), these details are ignored: the model is driven stochastically, there are only two possible states for each cell, and the earthquakes are generated according to simplified breaking rules.

Let us now explain the simplified view of earthquake generation that the model tries to sketch. In actual faults, the regional stress strains the rock blocks of the fault, making portions (patches) of the fault plane to become metastable. That is, they are static, but store enough elastic energy to propagate an earthquake rupture once triggered. Different processes (for example, aseismic creep and plastic deformation) dissipate stress along the fault plane, so stress is not directly converted into elastic strain. Earthquakes rupture some of the metastable patches of the fault, that then become stable, thus relieving strain. The hypocentre of an earthquake is usually located in a particularly strong patch of the fault plane, called “asperity” (Kanamori and Stewart, 1978; Aki, 1984; Das, 2003; Lei et al., 2003). Asperities appear to be persistent features where earthquake ruptures start once and again (Aki, 1984; Okada et al., 2003). Once the rupture starts, it propagates along the fault plane until it

arrives at a patch of the fault that is not sufficiently strained. Then the rupture cannot propagate further, and is arrested. The relatively stable patch that is not sufficiently strained and that arrests the rupture is called the “barrier” (Das and Aki, 1977; Aki, 1984; Das, 2003).

The model sketches these features as follows. It divides the plane of a fault into an array of equal cells, as depicted in Fig. 1. In previous papers (Vázquez-Prada et al., 2002, 2003; López-Ruiz et al., 2004; Gómez and Pacheco, 2004; González et al., 2004), this array was drawn vertically, in order to simplify its mathematical description. Here the model will be drawn horizontally, in order to sketch the fault plane in a way more similar to that of actual faults (which are usually longer along the strike than along the dip). Some other cellular automaton models discretize the fault plane in a similar way (e.g. Rundle et al., 2004). There is a total of N cells, each denoted by an index i . The parameter N is the only one that can be changed in the model. The cells can only be in one of two states: “empty” (stable) or “occupied” (metastable). The state of the model at each time step can be described simply by stating which cells are occupied and which are not. The increase of regional stress, as in other simple models (Bak and Tang, 1989; Newman and Turcotte, 2002; Castellaro and Mulargia, 2001; González et al., 2005), is represented by the random addition of “stress particles”. This randomness is a way of dealing with the complex stress increase in actual faults. At each time step, one cell is selected randomly, and a new particle arrives on it. That is, each cell has the same probability, $1/N$ of receiving the new stress particle. If the chosen cell is empty, the particle “occupies” it. This means that the regional stress has produced enough strain on that cell to make it metastable. If the cell is already occupied, that stress particle is lost; this is analogous to stress dissipation on the fault plane. The total number of occupied cells represents the total elastic strain on the fault.

In the model, we assume that the asperity is the first cell, $i = 1$, placed at one end of the array. This option is chosen because it simplifies the analytical description of the model. The stable cells act as barriers to earthquake rupture. When a stress particle fills cell $i = 1$, a rupture starts, and propagates through all the consecutive metastable cells until it is arrested by a stable cell. That is, if all the successive cells $i = 1$ to $i = k$ are occupied, and cell $k + 1$ is empty, then the effect of the earthquake is to empty all the cells from $i = 1$ to $i = k$. The other cells, $i > k$ remain unaltered. The cell $k + 1$ is a barrier: it is empty (stable), so the rupture cannot propagate through it. The size (rupture area) of the earthquake is k , the number of cells broken in the synthetic earthquake. Thus, the earthquake size in the model is discrete, $1 \leq k \leq N$. Earthquakes, in practice, are instantaneous in the model (they do not last for any time step). This represents the fact that earthquake ruptures are, indeed, much faster than the slow stress loading represented by the addition of particles.

The random addition of particles is what makes the model stochastic. It also

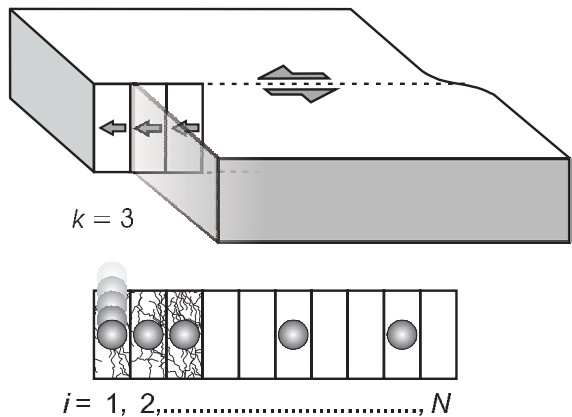


Fig. 1. The minimalist model as a sketch of a seismic fault. The fault plane is divided into an array of N equal cells, denoted with an index i , $1 \leq i \leq N$. The increase of regional stress is represented by the random addition of “stress particles” to the cells. Earthquake ruptures start at an asperity, the cell $i = 1$, when a stress particle arrives to it. The rupture propagates through all the consecutive metastable cells (occupied by particles). The rupture area is k , the number of cells broken. The figure depicts an earthquake with $k = 3$.

determines the rate at which earthquakes occur in the model. At each time step, independently of the previous earthquake history, there is a probability $1/N$ for the incoming stress particle to arrive at cell $i = 1$ and start an earthquake. Thus an earthquake, on average, occurs every N steps. The time between any two consecutive earthquakes is purely random (Poissonian, with rate $1/N$).

The cellular-automaton approach of this model is similar to that of the “forest fire” models, in which clusters of interconnected occupied cells (“trees”) “burn” and are reset to empty when they are randomly struck by “lightning” (Drossel and Schwabl, 1992; Henley, 1993). The utility of this kind of models for earthquake physics has been noted by Rundle et al. (2003). In the minimalist model there is no random “lightning”: the clusters of interconnected metastable sites are only emptied if they are connected to the cell $i = 1$ and if this fails.

2.2 Main properties of the model

In this section, we will briefly review some properties of actual seismic faults that the minimalist model, despite its simplicity, is able to reproduce. The minimalist model, of course, lacks the detailed description of the seismic process that a fully dynamical model can display. For example, it does not include the effects of fault friction, elastic stress transfer, or the role of fluids that more complex models can take into account. This detailed description, as noted before, was sacrificed in order to simplify the model analysis.

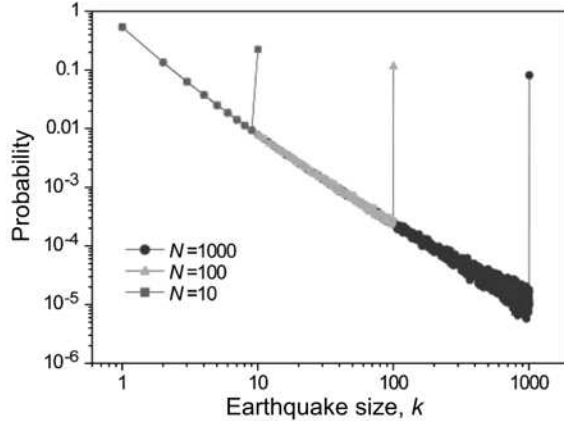


Fig. 2. The size-frequency distribution of earthquakes in the minimalist model. The earthquake size (rupture area) is k , the number of cells broken by the earthquake. The magnitude would be proportional to the logarithm of k . The curves for any N overlap, except for the characteristic earthquakes (with $k = N$). The distributions shown are for $N = 10$, 100 and 1000.

In the previous subsection we already noted some similarities between the model and actual faults that were looked for when designing the model. Apart from these, the minimalist model spontaneously displays some other characteristics that can be compared with those of actual faults: the earthquake size-frequency distribution, the pattern of strain loading on the fault, the seismic quiescence, the duration of the earthquake cycle, and the stress shadow.

2.2.1 Earthquake size-frequency distribution

The size-frequency distribution of earthquakes in the minimalist model (Fig. 2) is an example of the so-called characteristic earthquake distribution (Wesnousky et al., 1983; Schwartz and Coppersmith, 1984; Youngs and Coppersmith, 1985; Wesnousky, 1994). In this distribution, the small and medium-size shocks follow a power law, while the maximum-size events ($k = N$ in the model), have a distinctly higher frequency than the extrapolation of this power law would indicate. This kind of distribution is shown by earthquakes in at least some seismic faults (Stirling et al., 1996). For a discussion of this distribution and the insight gained with the minimalist and other models, see Appendix A.

The most widely used scale of earthquake magnitudes is the moment magnitude, which is proportional to the logarithm of the rupture area (Kanamori and Anderson, 1975). For this reason, we use a logarithmic scale for k in Fig. 2. In this figure it can also be seen that the probability of the characteristic earthquake depends on N , while the probability of smaller earthquakes ($k < N$) overlap for models with different N (Vázquez-Prada et al., 2002). For a detailed description of the tendency of the size-frequency relationship of events when the system size grows to infinity, see López-Ruiz et al. (2004).

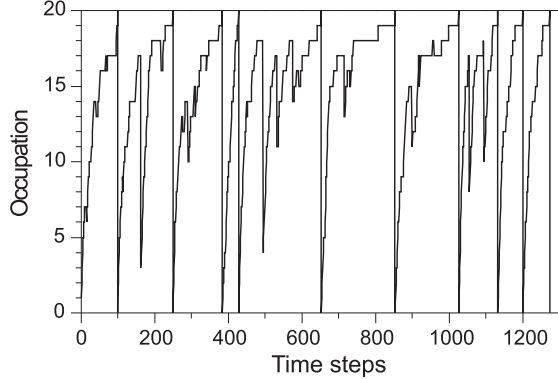


Fig. 3. The number of occupied cells in a minimalist model with $N = 20$, for ten seismic cycles. This number is analogous to the total elastic strain accumulated in the fault. Sudden drops correspond to earthquakes. Each seismic cycle ends with an earthquake of size N .

2.2.2 Pattern of strain loading

On actual faults, the strain does not accumulate uniformly along the seismic cycle. Instead, the strain loading rate is faster just after a large earthquake, and decreases over time (Michael, 2005). In the minimalist model, a similar effect is observed (Fig. 3). The total elastic strain in the model is represented by the occupation, that is the total number of occupied cells. Just after a large earthquake, this number increases rapidly, and then more slowly. The cause is that when more cells are occupied, it is less probable for the incoming stress particles to land on empty cells. This pattern can be complicated by intermediate, non-characteristic earthquakes. Just before the next characteristic earthquake, the occupation reaches a steady state (“plateau”), which gives rise to the next property of the model.

2.2.3 Seismic quiescence

On actual faults, a period of reduced seismic activity, called seismic quiescence, is observed during months or years before many mainshocks (Wyss and Habermann, 1988; Scholz, 2002). As mentioned above, the number of occupied cells in the minimalist model reaches a plateau just before each characteristic earthquake (Fig. 3). Once this plateau starts (when $N - 1$ cells, from $i = 2$ to $i = N$, are occupied), only the characteristic earthquake can be produced, and, on average, N time steps have to elapse until a stress particle hit the asperity cell ($i = 1$) and generates the earthquake. Thus, the average duration of the plateau with seismic quiescence is N time steps.

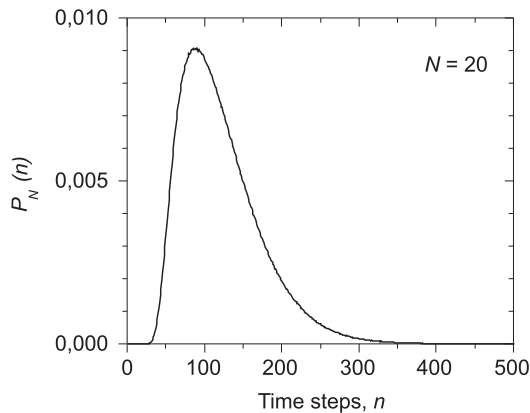


Fig. 4. The discrete distribution function of the duration (in time steps, n) of the seismic cycle in a minimalist model with size $N = 20$. Note that cycles shorter than N time steps cannot occur.

2.2.4 Duration of the earthquake cycle

The earthquake cycle of a fault is the time between two consecutive large earthquakes that rupture the whole fault or most of it (e.g. Scholz and Gupta, 2000). These quakes that break most of or all the fault are called characteristic earthquakes (Schwartz et al., 1981; Coppersmith and Schwartz, 1983; Wesnousky et al., 1983; Schwartz and Coppersmith, 1984). In the model, the characteristic earthquakes are those that rupture the N cells. These are the ones we will try to forecast later on. The seismic cycle in actual faults is not periodic. The times between large earthquakes follow a certain statistical distribution which is still not well known. There are several distributions able to describe the recurrence of large earthquakes (e.g. gamma, lognormal, Weibull, Brownian passage time; Michael, 2005), and the distribution of the seismic cycles in the minimalist model is one of them.

In the model, the number of time steps (particle throws) elapsed since the last characteristic earthquake is called n . The duration of the seismic cycles is statistically distributed according to a discrete probability distribution, that depends on N and is denoted $P_N(n)$. This distribution is well known. It can be analytically derived for models with small N (Gómez and Pacheco, 2004). For any N , it can be measured in detail by simulating numerically the evolution of the model during some millions of seismic cycles. This distribution is useful for describing the recurrence of large earthquakes on actual faults (Gómez and Pacheco, 2004). It is drawn for $N = 20$ in Fig. 4. Note that the consecutive earthquakes of any size in the model take place according to a purely random, Poisson distribution, but that the time distribution of earthquakes of a specific size is not Poissonian, as this depends on the size and time of occurrence of the previous events. As a specific case, the distribution of characteristic earthquakes, $P_n(N)$ is not Poissonian. This is discussed further in the next subsection.

2.2.5 Stress shadow

When a fault generates a large earthquake, the elastic strain is reduced, and a minimum time has to elapse until the fault, by slow tectonic deformation, accumulates enough strain to generate another large earthquake. This effect is called stress shadow (Harris, 2000). In the minimalist model there is a stress shadow: if an event of size k takes place, at least k time steps have to elapse before another event of that size can occur. As a specific case, if a characteristic earthquake takes place, at least N time steps have to elapse before the next characteristic earthquake.

3 General scheme of forecasting

In this section we will explain the general framework for the forecasting of the largest earthquakes in the model. As a first remark, we have to consider that the model is stochastic, so it is not predictable with absolute precision. Only simple deterministic systems are fully predictable. The evolution of complex systems, such as the atmosphere or the lithosphere (even if it were deterministic) is very sensitive to the initial conditions. As these complex systems cannot be fully characterized, they turn out not to be fully predictable either.

Earthquake prediction (Keilis-Borok, 2002; Keilis-Borok and Soloviev, 2003; Rundle et al., 2003), as well as some atmospheric predictions (Mason, 2003), is frequently regarded as a binary forecast: one has to decide whether a large earthquake is going to occur or not, in a certain time-space window, instead of calculating the exact probability of this event. In this binary-forecasting approach, an “alarm” is declared when a large earthquake is expected. If it takes place when the alarm is on, the outcome is a successful forecast. If it takes place when the alarm is off, there has been a prediction failure. If the alarm was declared during a certain period, but the expected earthquake did not happen, that constitutes a false alarm.

Note that for using this approach it is necessary to define precisely what the target earthquakes are that we wish to forecast. Usually they are defined as those with a magnitude larger than a given threshold, both when dealing with actual earthquakes (Keilis-Borok and Soloviev, 2003; Rundle et al., 2003) or with synthetic ones (e.g. Pepke and Carlson, 1994; Hainzl et al., 2000). In the minimalist model, it is natural to choose as target events the characteristic earthquakes (size $k = N$), as they mark a distinct peak in the size-frequency diagram, being much more frequent than other large earthquakes.

A way to quantify the forecasting ability of a certain strategy is to compute the fraction of errors, f_e , and the fraction of alarm time, f_a (Molchan, 1997).

Given a certain time series of the model, f_e is the ratio of the total number of prediction failures to the total number of target events. And f_a is the ratio of the total time during which the alarm was on to the total duration of the time series. The fraction of false alarms, f_f , is included in f_a , and is the ratio of the total duration of false alarms to the total duration of the time series.

Of course, a good forecasting strategy should render small f_a , f_e and f_f . However, as a general rule, a strategy that renders low f_e tends to produce large f_a and f_f . Dealing with real seismicity, both a failure and an alarm are costly. Eventually, decision-makers would need to consider what is less costly: to predict most of the dangerous earthquakes, but declaring many alarms, or to declare fewer alarms but failing the forecast of more large shocks (Molchan, 1997). Depending on the trade-off between costs and benefits, one should try to minimize a loss function, L , that can depend on f_a , f_e and/or f_f .

In the next section, we will describe the forecasting strategies that we will use to compare the merits of the new strategy proposed in this paper, based on synchronizing models between themselves. In the first of the subsections we will indicate the loss function we will try to minimize in the forecasting of the model.

4 Forecasting strategies for comparison

We describe three forecasting strategies, based on the earthquake series, that we will use to assess the merits of the new strategy described later in this paper. The first two strategies (the random guessing strategy and the so-called reference strategy) can be used in any system. The third is specific to the minimalist model, and serves to ideally determine its maximum theoretical predictability.

4.1 *Random guessing strategy*

In this strategy, the alarm is randomly turned on and off, during a certain fraction of alarm time, f_a . It is simple to apply this strategy to any cellular automaton model. Here, in each time step, the alarm is on with a probability p . As a result, the alarm will be on during a fraction p of time steps ($f_a = p$). When the target earthquake finally occurs in a certain time step, there will be a probability p for the alarm to be on. Thus, on average, a fraction p of target earthquakes will be predicted, and a fraction $f_e = 1 - p$ will be prediction failures, so $f_a + f_e = 1$. This strategy has two trivial cases: if the alarm is always on ($f_a = 1$), all the target earthquakes are “forecasted” ($f_e = 0$).

Conversely, if the alarm is always off ($f_a = 0$), we fail to predict any of them.

To be statistically significant, any forecasting strategy must render better results than a random guess. A natural way to measure this improvement is to consider the loss function $L = f_a + f_e$. Then, $L = 1$ means that the strategy performs as a random guess, and $L = 0$ means a perfect prediction. If $L > 1$, the strategy is performing exactly the opposite to how it should. Thus, the exact reverse strategy should be considered, and this will provide the opposite results ($f'_a = 1 - f_a$, and $f'_e = 1 - f_e$).

4.2 Reference strategy

Of course, the random guessing strategy depicted above is only useful as a baseline, but does not serve to provide a real significant forecast. In this subsection we describe the simplest meaningful forecasting strategy one can consider for any system. This will be called the reference strategy, and any forecasting procedure more complex than this should render better results.

The reference strategy consists simply in declaring an alarm some time after each target event, and maintaining it on until the next target event (Newman and Turcotte, 2002; Vázquez-Prada et al., 2003; González et al., 2005). As a general rule, the shorter this time, the bigger f_a and the lesser f_e . Which time is best, then? For the minimalist model, we can look for the number of time steps n to use with this strategy for obtaining a lesser L . In a previous paper (Vázquez-Prada et al., 2003) we observed that effectively, for each N , there is a n that minimizes L . In Fig. 5, the minimum L that can be obtained with this strategy is plotted for N between 2 and 20, in the curve labeled “Reference”. This method does not generate any false alarm, nor take into account the occurrence of earthquakes smaller than the characteristic ones. The only information required is $P_N(n)$, the probability distribution function of the duration of the cycles (Vázquez-Prada et al., 2003). Taking into account smaller earthquakes, the forecast can be modestly improved in the model (Vázquez-Prada et al., 2003).

4.3 Ideal strategy

As the minimalist model is very simple, it is possible to explore its maximum predictability. The ideal strategy needed for getting this result, unlike the two previously described, is model-specific. It is deduced in Appendix B. This ideal result could only be obtained if we could “see” inside the model to check at each time step which cells are occupied and which are not. Thus it requires a perfect knowledge of the system, and equivalent strategies cannot be used

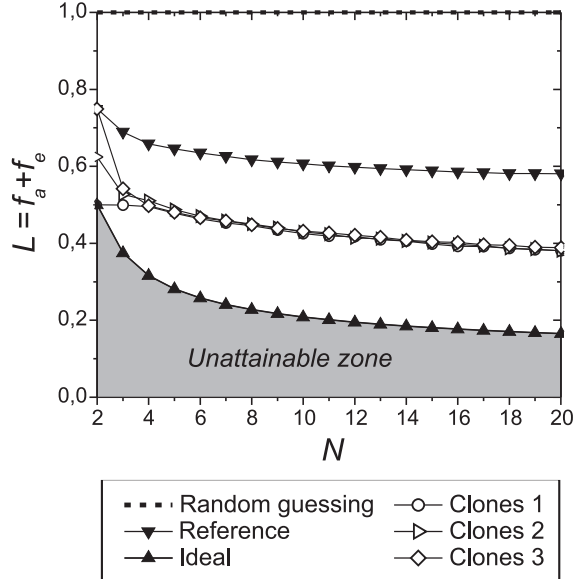


Fig. 5. Loss function (L) obtained with the different forecasting methods used in this paper, for various system sizes ($2 \leq N \leq 20$). A random guessing strategy would render $L = 1$ for any N , while $L = 0$ would mean a perfect prediction. The shadowed zone is unattainable for any forecasting strategy used in the minimalist model, and the strategy that marks its upper limit is called “Ideal”. The “Reference” strategy is based only on the series of the largest earthquakes in the model. The three strategies labelled “Clones” are based on the synchronization of models with the minimalist model whose largest earthquakes we try to forecast.

with actual faults where we cannot know the detailed state of stress and strain. In Appendix B it is deduced that the alarm should be declared at the instant in which $N - 1$ cells of the model are full (just at the beginning of the plateau commented on in Section 2.2.3). Then, it should be maintained on until the next characteristic earthquake. This is a no-error strategy ($f_e = 0$, and $L = f_a$). As the model is stochastic, f_a is not zero; a minimum alarm time is needed to forecast all the characteristic earthquakes. It is given by $f_a = L = N/\langle n \rangle$, where $\langle n \rangle$ is the average duration of the cycles (which depends on N). This L is also plotted in Fig. 5, in the curve labelled “Ideal”. This is the rigorous minimum L that can be obtained in the model. A good forecasting strategy should produce a L lesser than the “Reference” curve and as close as possible to the “Ideal” curve.

5 Synchronization-based forecasting

In this section we will describe the novel forecasting method based on the synchronization between models, obtained by imposing the rupture area of a minimalist model onto other similar models. This section expands and complements our previous results (González et al., 2004).

We will try to forecast the characteristic earthquakes generated by a minimalist model with N cells. This model will be called *master*. We will consider this master as if it were an actual fault, from which we can know the rupture area of its earthquakes (equivalent to the number of cells broken, k), but not the strain or stress at depth (equivalent to the occupation state of the model cells). As in an actual fault, we cannot change the state of the master at any moment.

In this forecasting approach we will use other models, which we call *clones* (González et al., 2004). These are equivalent to the models that a scientist devises for forecasting the future evolution of the fault. We will modify their evolution at will, and their governing rules will be different than those of the master. In this paper, for simplicity, we will consider that the clones are also arrays of N cells. The average duration of the earthquake cycle in the model (average recurrence interval of the characteristic earthquakes), $\langle n \rangle$, strongly depends on N (Gómez and Pacheco, 2004). Choosing a different N for the clones will imply a different loading rate of the cells and a different average recurrence interval of the characteristic earthquakes in the clones than in the master. These effects would require further tuning of the clones, which would complicate the following discussion.

Let us describe in the following paragraphs the general outline of the procedure. We will use a total of Q clones, that will be loaded (one particle per time step and per clone) at the same time as the master, but randomly and independently to the master and to each other. We will apply some procedures for partially synchronizing the clones with the master. If in a given time step the master does not generate any earthquake, we will oblige the clones not to generate any earthquake either. If the master does generate an earthquake, we will force the clones to reproduce the rupture area of this earthquake, as described below in more detail. Note that, although the master and the clones are driven simultaneously, the effects of the master are dealt with first.

Why use several clones? The master and the clones are all stochastic, so each one evolves with time in a different way. By using several clones, we can take into account a broad range of possible evolutions. By using only one clone, we could not be very sure that it is satisfactorily mimicking the evolution of the master. However, if several of these Q clones are in the same state, then it is more probable that the master is also in that state. If the clones were deterministic, only one would be required.

We have commented before (Section 4.3 and Appendix B) that the ideal forecasting strategy for the minimalist model will be to declare the alarm just when $N - 1$ cells of the model become occupied. Then the master enters the stage of seismic quiescence, or plateau, and the next earthquake is the characteristic one. We will try to determine this ideal instant as well as possible

with the clones. For this, we will use a “democratic” procedure: we will declare an alarm when a minimum of q clones “vote” (become occupied to a certain threshold, described below). Later on we will explore the combinations of Q and q that render the best results. Once the alarm is declared, it is maintained on until the next earthquake in the master. If it is a characteristic one, this is a successful prediction. Its rupture is imposed on the clones (so we reset all the cells of the clones to empty) and a new cycle starts. If the next earthquake is not a characteristic one, this represents a false alarm. We will disconnect the alarm, and impose the rupture on the clones as is done with any other earthquake. Of course, if a characteristic earthquake takes place when the clones have still not declared the alarm (when less than q clones have voted), this is a prediction failure. If the clones declare an alarm in the same time step in which the master generates a characteristic earthquake, we also consider this as a prediction failure.

We will follow three approaches, each implying a lesser knowledge of how the master model works. They are depicted in Fig. 6 and described as follows:

- (1) This first approach will indicate which is the best result that can be obtained with this synchronization-based forecasting. For this reason, the clones are indeed minimalist models identical to the master (González et al., 2004). We assume as known that, just after an earthquake with rupture area k , the first $k + 1$ cells in the master, for sure, are stable (the k just broken plus the one that acts as a barrier for the rupture). Thus, if the master generates an earthquake of size k , we will reset to empty the first $k + 1$ cells of the clones. We also consider as known that the cell $i = 1$ is the asperity that triggers the ruptures. So if the master does not generate any earthquake, the particles in the clones will be randomly thrown to the cells $i \geq 2$, thus precluding any earthquake in the clones. A clone votes when $N - 1$ of its cells are full.
- (2) In this second approach, we are more ignorant about how the master works. We do not know where the asperity nor the barrier that stops the rupture are placed; we only know which cells have ruptured. If the master generates an earthquake of size k , we will reset to empty only the first k cells of the clones. If it does not generate an earthquake, we will throw the stress particles to any of the cells in the clones. A clone votes when its N cells are full.
- (3) In the third approach, we only know the size of the earthquake, and thus its rupture area k , but not exactly which cells of the master have ruptured in the earthquake. If there is an earthquake in the master, we will randomly empty k occupied cells of each clone. If the clone has less than k occupied cells, all are emptied. If the master does not generate an earthquake, we will throw the stress particles to any of the cells in the clones. A clone votes when its N cells are full. In this approach the position of the cells in the clone are irrelevant. Each clone is thus

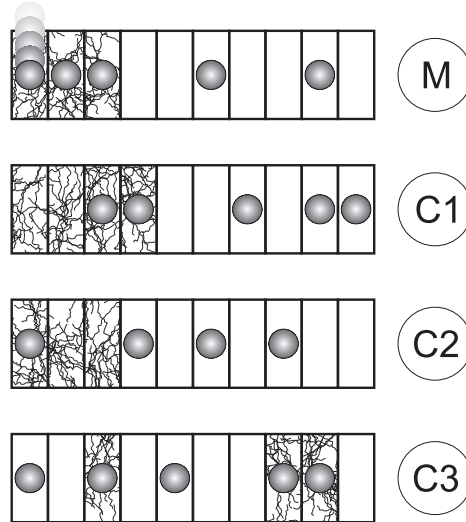


Fig. 6. Sketch that shows how the rupture area of an earthquake in the master model (M) is imposed on the clones (C), for each of the three synchronization-based approaches. In this example, the master generates an earthquake with rupture area $k = 3$. In the first approach (C1), the first $k + 1$ cells rupture and will be reset to empty. In the second one (C2), this occurs only with the first k cells. In the third approach (C3), this happens to k occupied cells chosen randomly. The first cell of the clones can be occupied only in the second and third approaches.

equivalent to the so-called box model (González et al., 2005).

Note that, ideally, the clones should have the same number of occupied cells as the master. For this reason, as a way to measure the degree of synchronization between a clone and the master, we used (González et al., 2004) the fraction of time, τ , during which both of them have the same number of occupied cells. If two independent masters run simultaneously, they have the same number of occupied cells, just by chance, during a certain τ . When a clone and a master are compared, this τ greatly increases, as shown in Fig. 7: partial synchronization is achieved. The best results, as expected, are achieved with the first of the three approaches.

The results of f_a , f_e , f_f and $L = f_a + f_e$, for different values of Q and q can be plotted as in the diagrams of Fig. 8. In this figure we have plotted only results corresponding to the first of the three approaches and $N = 20$, but similar figures, with the same overall properties, can be drawn for the other two approaches and for any N . There are simple trends in these graphs. In Section 3 we noted that, in general, a forecasting strategy that produces lower f_e tends to produce higher f_a and f_f . If Q is fixed (same row), the greater the q , the later the alarm is declared, so f_a and f_f are lesser and f_e is greater. If q is fixed (same column), the greater the Q , the earlier the alarm is declared, resulting in the opposite trend.

We are interested in finding the combinations of Q and q that minimize L .

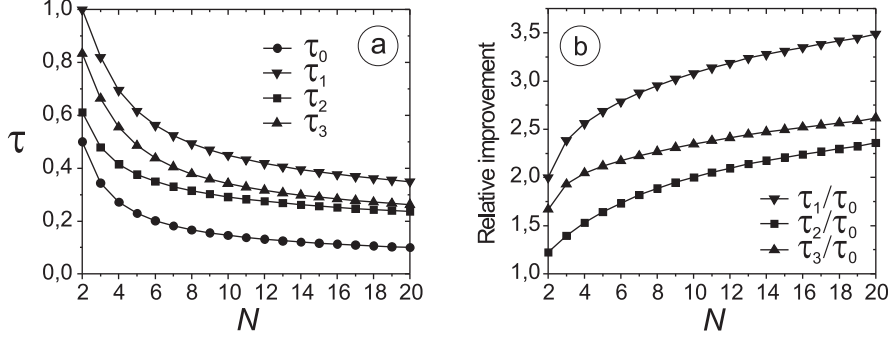


Fig. 7. **(a)** The fraction of time, τ , during which two models have the same number of occupied cells. This depends on whether they are two independent masters (τ_0) or a master and a clone (governed by one of the three different synchronization approaches: τ_1 , τ_2 and τ_3). **(b)** The relative improvement, defined as τ_n/τ_0 .

The interesting fact is that the sum $f_a + f_e$ shows a rectilinear “valley” for certain combinations of Q and q , marked with squares in the graph of Fig. 8. This valley goes down as Q and q increase. In Fig. 9 it can be observed that the valley goes down indefinitely, tending to a lowest asymptotic value of L . We estimate this value, as a function of Q , with a three-parameter exponential fit of the form $F = a \exp[b/(Q + c)]$, where a , b , and c are parameters. The value of a is the asymptotic one for $Q \rightarrow \infty$. This value is represented, for each N , in Fig. 5. The f_a , f_f and f_e also have asymptotic trends along this valley of L , also plotted in Fig 9. They can also be fitted with the same kind of three-parameter distribution, to estimate their asymptotic values as $Q \rightarrow \infty$. A nice property is that, as shown in Fig. 9 for a certain case, these forecasting approaches predict most of the characteristic earthquakes (f_e is low), and have a very small fraction of false alarms.

As can be noted in Fig. 5, the minimum L obtained for the three different approaches is almost the same, so the optimizing procedure based on choosing Q and q counteracts the different performance of single clones, depicted in Fig. 7. The second and third approaches give only slightly greater L than the first one. The differences are large only for small N s. Another difference, not shown in the figures, is that L decays to its asymptotic value more slowly in the second and third approaches than in the first one. That is, they need more clones than in the first approach to achieve a given low L . This is because the first approach synchronizes more efficiently each individual clone with the master (Fig. 7). In any case, around thirty to forty clones already give a result very close to the asymptotic one. Note how the strategy performs much better than a random guess, and also much better than the reference strategy described in Section 4.2. Its results are intermediate between the ideal forecast and the reference one.

Another way to measure the synchronization of the clones with the master is drawn in Fig. 10. The ideal strategy (Section 4.3 and Appendix B), would be

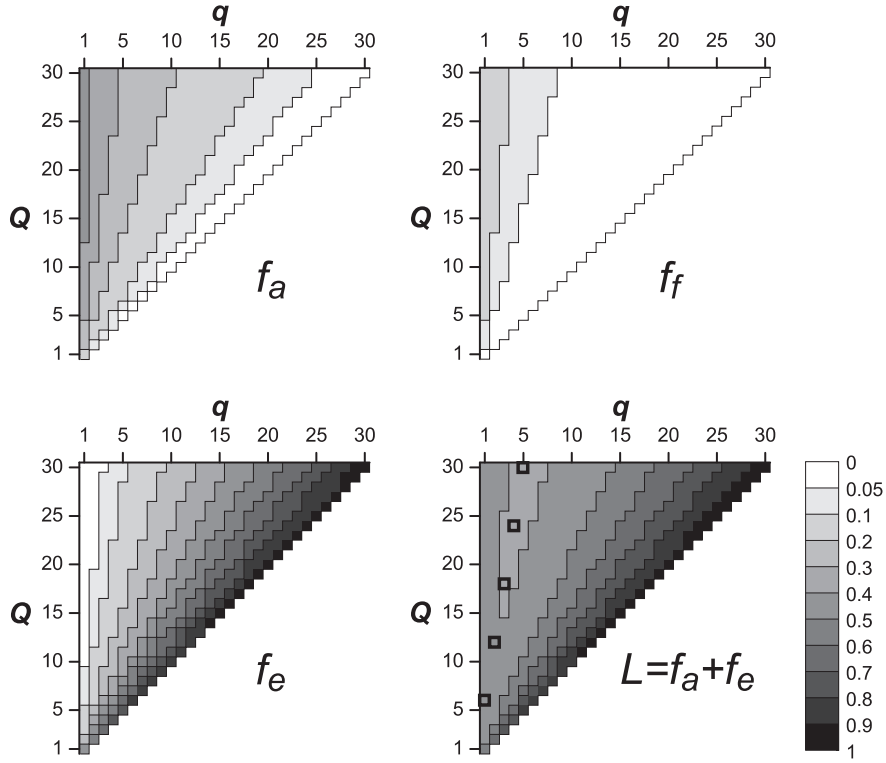


Fig. 8. Fraction of alarm time (f_a), fraction of false alarm time (f_f), fraction of errors (f_e), and loss function (L) obtained with the the first synchronization-based forecasting approach, for $N = 20$ and different numbers of clones (Q) and votes (q). The squared cells mark a rectilinear valley in the values of L .

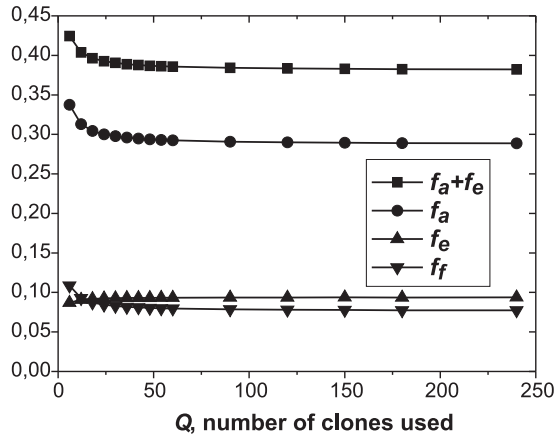


Fig. 9. Loss function (L), fraction of alarm time (f_a), fraction of false alarm time (f_f) and fraction of errors (f_e) obtained with the first synchronization-based forecasting approach, for $N = 20$ and different numbers of clones (Q) along the rectilinear valley observed in L in Fig. 8 (the first five points of each curve correspond to the cells marked in that figure).

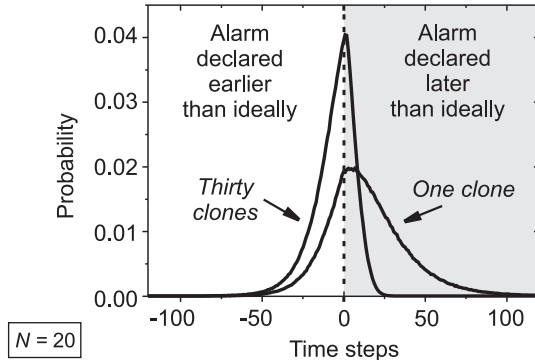


Fig. 10. Probability that a clone or thirty clones (with $q = 5$; the uppermost squared cell in L in Fig. 8) declare an alarm in a given time, around the instant when it should for obtaining the ideal forecast.

to declare the alarm just when $N - 1$ cells of the master are full. The figure shows how a single clone connects the alarm around that moment, but a group of clones does a much better job.

6 Discussion and conclusions

In this paper we have tried to provide some insight into how to synchronize numerical models with seismic faults, in order to better forecast large earthquakes in them. The idea is that, although we can rarely measure the stress and strain in actual faults, we can estimate the rupture area and coseismic displacement of their earthquakes. If we force a calibrated model to reproduce every earthquake rupture of the fault it simulates, probably the model will be synchronized with the fault. Then it could be used to forecast the future evolution of the fault, including future large earthquakes. This idea is not completely new: e.g. Ward (2000) forced a model to reproduce a large-earthquake rupture and run the model forward to see what could happen in the future. The results of this paper expand on earlier ones (González et al., 2004), and are still only theoretical, but fully quantitative. We demonstrate that it is possible to partially synchronize numerical fault models between themselves, and use this to forecast synthetic earthquakes.

One of the models, called the master, evolves freely. We consider it as an actual fault, from which we can know the rupture area of its earthquakes, but not the strain or stress at depth. Our goal is to forecast the largest earthquakes it generates. In the synchronization-based forecasting, we use several other models, called clones, similar to the master (calibrated to have the same average recurrence interval of large earthquakes that the master has). These clones are equivalent to the models that can be devised to simulate a seismic fault. They are run simultaneously and independently to the master and to each other. We

force them to reproduce the series of earthquake ruptures of the master, and this makes them partially synchronized with it. In simple words, if the master does not generate an earthquake, we preclude any earthquake in the clones; if the master does generate an earthquake, we impose the same rupture area on the clones. When several of the clones indicate that a large earthquake is impending in the master, we declare an alarm. This efficiently predicts most of the largest earthquakes of the master, with a relatively low fraction of total alarm time and few false alarms. These results are robust; they are almost the same when the exact rules for imposing the earthquake ruptures vary. This synchronization-based forecasting outperforms other procedures based only on the earthquake series of the model.

The master and the clones are stochastic (random), so each individual clone is only partially synchronized with the master. However, when several clones are in the same state, then it is more likely that the master is also in this state, so the group of clones makes a much better forecasting job than only one clone does. If the clones were deterministic, as a general rule only one would be needed; more clones would have identical evolutions if run with the same initial conditions.

The procedure developed here is a kind of *ensemble* forecasting, in which several models are run to obtain a better picture of how a system will evolve. This concept is used in atmospheric forecasting (Palmer et al., 2005): several models are run simultaneously, and their average result has a larger forecasting ability than that of an individual model (Houghton, 2002; Palmer et al., 2005). Each model in this approach has slightly different initial conditions, to take into account measurement errors and then to represent one possible state of the atmosphere, among various possibilities. In our approach, each clone marks a possible state of the master among a range of possible options. Several deterministic clones could also be used with different initial conditions.

Our procedure also shares some similarities with certain earthquake forecasting algorithms (Kossobokov et al., 1999; Keilis-Borok and Soloviev, 2003), in which several seismicity functions are evaluated in real time. When several of these functions indicate that a large earthquake is probable, an alarm is declared. In our approach, the clones are performing a role similar to these functions, monitoring what is happening in the master.

Our theoretical proposal is that a possible way to synchronize more complex, calibrated models with real faults might be to force them to reproduce the past series of earthquakes (with the same rupture area and/or coseismic displacement). This would need to be tested in the future. Also it will be possible to test whether this procedure works in the forecasting of synthetic earthquakes in other models.

Forcing the models to reproduce only one large observed rupture (as in Ward, 2000) probably is not enough (this is certainly the case in our stochastic model). Complex and chaotic systems, such as the lithosphere, are very sensitive to initial conditions. Forcing the model to reproduce only one rupture is a necessary and laudable first step, but probably does not constrain the initial conditions sufficiently. We propose that every observed rupture, albeit small, should be considered. Small earthquakes are much more frequent than large ones, thus providing much more data. Moreover, they provide insight into the mechanical state of the crust (Seeber and Armbruster, 2000) and into the mechanics of earthquake rupture (Rubin, 2002). Their location may indicate the patch of the fault plane which is experiencing higher stresses and is likely to rupture in the next large shock (Schorlemmer and Wiemer, 2005). Finally, they are important in the transfer of stress within the lithosphere, and in earthquake triggering (Helmstetter et al., 2005).

7 Acknowledgments

Á.G. thanks Robert Shcherbakov for helping him to view the model with new eyes. We are also grateful to the University of Zaragoza Institute of Bio-computation and Physics of Complex Systems (BIFI) for allowing us to use their supercomputing facilities. The Spanish Ministry of Science and Education funded this research by means of the project BFM2002-01798, and the grant AP2002-1347 held by Á.G.

A Size-frequency distributions of earthquakes in faults

This appendix deals with two distributions proposed in the literature for the size-frequency relationship of earthquakes in faults: The Gutenberg-Richter and the characteristic earthquake distributions. We also give some insights gained from the minimalist and other numerical models on this topic.

It is generally considered that the regional seismicity of large enough geographic areas, averaged during long enough time intervals (Molchan et al., 1997), follows the Gutenberg-Richter law (Ishimoto and Iida, 1939; Gutenberg and Richter, 1944, 1954),

$$\log N_{GR}(> m) = -bm + a, \tag{A.1}$$

where N_{GR} is the cumulative number of earthquakes with a magnitude greater than m occurring in a specified area and time and b and a are empirical

parameters. This relation holds for a certain magnitude interval, and is a power law when magnitude is expressed in terms of rupture area (Aki, 1981):

$$N_{GR}(> A) = CA^{-b}, \quad (\text{A.2})$$

where N_{GR} is the cumulative number of earthquakes with rupture area greater than A occurring in a specified area and time, and C is an empirical parameter. The b -value, common to both equations, varies from one region to another, generally within the range $0.8 < b < 1.2$ (Frohlich and Davis, 1993), and also may depend on the depth of the hypocentres considered (Molchan et al., 1997; Kagan, 1999; Gerstenberger et al., 2001).

However, the Gutenberg-Richter law may not hold for the seismicity particular to a single fault or fault segment. At the beginning of the 1980's, certain geologic investigations led to the hypothesis that most of the seismic moment on a fault or fault segment is released by repetition of the largest earthquakes it can produce, given its area. Such earthquakes were called characteristic (Schwartz et al., 1981; Coppersmith and Schwartz, 1983; Wesnousky et al., 1983; Schwartz and Coppersmith, 1984). This characteristic-earthquake model for earthquake recurrence on faults is one possible option among other alternatives (Scholz, 2002), and is frequently assumed in many seismic hazard studies. In the characteristic-earthquake size-frequency distribution, that suggested for individual faults according to this model (Wesnousky et al., 1983; Schwartz and Coppersmith, 1984; Youngs and Coppersmith, 1985; Wesnousky, 1994), only small earthquakes would follow the Gutenberg-Richter law. The frequency of medium-sized events would be very low, or they might even be absent. However, the frequency of the characteristic earthquakes would be higher than that estimated by extrapolating the Gutenberg-Richter distribution of the smaller events.

Later studies added further support to this hypothesis (e.g. Wesnousky, 1994; Stirling et al., 1996; Sieh, 1996), and raised debate on the topic (Kagan, 1996; Wesnousky, 1996). There is also concern over the possibility that poor statistics of large earthquakes could produce artifacts in the size-frequency distributions (Stein and Newman, 2004). Numerical models can generate as many synthetic earthquakes as desired, and thus overcome these sampling problems. Some insights into real seismicity (Stirling et al., 1996) and into numerical models (e.g. Rundle and Klein, 1993; Main, 1996; Dahmen et al., 1998; Steacy and McCloskey, 1999; Moreno et al., 1999; Hainzl and Zöller, 2001; Heimpel, 2003; Zöller et al., 2005) have indicated that the heterogeneity of the fault system may influence the shape of the size frequency distribution of earthquakes: fault systems with complex traces and models with heterogeneous fault planes tend to display Gutenberg-Richter distributions, while faults with simple geometry and models with low heterogeneity tend to display characteristic-earthquake behavior. In general, earthquake ruptures can span all or most

the fault plane if this is homogeneous, while the barriers in an heterogeneous plane tend to arrest the rupture, preventing it from spanning the whole plane. Aki (1984) also noted that the characteristic earthquakes appear to be associated to those faults with a relatively homogeneous fault plane with stable asperities. This may be the case of the minimalist model, where all the cells have the same properties, and earthquakes always start in the same asperity.

The characteristic earthquakes, in which all or most of the fault plane breaks, are also possible because the faults are finite (e.g. Heimpel, 2003). Characteristic earthquakes are thus a certain finite-size effect. This is also true for the minimalist model, where the probability of the characteristic earthquake tends to zero as the system size (N) grows (López-Ruiz et al., 2004).

In large enough geographic regions, encompassing a large enough number of active seismic faults, the Gutenberg-Richter law can result from the addition of the characteristic-earthquake distributed seismicity from each fault (Wesnousky et al., 1983; Molchan et al., 1997), if the distribution of fault sizes and fault slip rates is taken into account (Wesnousky et al., 1983). This was also checked in the minimalist model. Fault sizes in Nature are distributed according to a power law (fractal) distribution. A population of non-interacting minimalist models whose N s follow this fractal scaling generates Gutenberg-Richter distributed seismicity (López-Ruiz et al., 2004).

B Deduction of the ideal forecasting strategy

In this appendix we will deduce the ideal strategy outlined in Section 4.3. This strategy renders the lowest (best) value of $L = f_a + f_e$ achievable in the minimalist model.

For this reasoning we would consider every cycle of the model as composed of two independent and consecutive stages. The first, that will be called the *loading* stage, starts just after the occurrence of a characteristic earthquake. During this stage the total number of occupied cells grows, but not in a monotonic way, because the particles may land in already occupied cells (and then be dissipated), and also because of the occurrence of non-characteristic earthquakes. As commented on in Section 2.2.2, during this first stage, the occupation grows faster when none or few of the cells are occupied, that is, after a large earthquake, and more slowly when many cells are occupied, because it is less probable for the stress particles to arrive at empty cells. When $N - 1$ cells (all but the first one) become occupied, this first stage ends and the second stage, that will be called the *hitting* stage (or *plateau* in the occupation), starts. In this second stage, the system resides statically in the state of maximum occupancy until a particle arrives at the first cell. Then, a characteristic

event occurs, all the cells are emptied, and a new cycle begins. The hitting stage can be mathematically treated as a form of Russian roulette.

Both the time spent by the system in the loading stage, x , and in the hitting stage, y , are statistically distributed. The distribution of y , denoted by $P_2(y)$, is geometric. Considering that, in each time step, the probability of hitting the first cell is $p = 1/N$, and its complementary is $q = 1 - 1/N$, it follows that

$$P_2(y) = \frac{1}{N} \left(1 - \frac{1}{N}\right)^{y-1}, \quad (\text{B.1})$$

whose mean is

$$\langle y \rangle = N, \quad (\text{B.2})$$

and whose standard deviation is

$$\sigma = N \sqrt{1 - \frac{1}{N}}. \quad (\text{B.3})$$

The time elapsed between consecutive characteristic events has been denoted by n , which is statistically distributed according to the function $P_N(n)$. Keeping this notation, and bearing in mind that the variables x and y are independent, results in

$$\langle n \rangle = \langle x \rangle + \langle y \rangle. \quad (\text{B.4})$$

That is, the mean length of the cycles $\langle n \rangle$ is the sum of the mean lengths of the two stages.

It is clear that the best L would be obtained *only if* we knew the state of occupation of the system and could mark, for each cycle, the instant at which the stage of loading concludes. In this case, $f_e = 0$, but because the hitting stage is completely stochastic, f_a (and thus L) cannot be nil.

Let us explore the result of L obtained if we turn the alarm on at a given value $y = y_0$ within the second stage of all the cycles. With this strategy, the fraction of errors is given by

$$f_e(y_0) = \sum_1^{y_0} P_2(y), \quad (\text{B.5})$$

and inserting Eq. B.1 we obtain

$$f_e(y_0) = 1 - q^{y_0}. \quad (\text{B.6})$$

With respect to to the fraction of alarm, its form is

$$f_a(y_0) = \frac{\sum_{y_0}^{\infty} (y - y_0) \cdot P_2(y)}{\langle x \rangle + \langle y \rangle}, \quad (\text{B.7})$$

and inserting Eq. B.1, we get

$$f_a(y_0) = \frac{Nq^{y_0}}{\langle x \rangle + N}. \quad (\text{B.8})$$

Note the important contribution of the first stage of the process in the denominator. Thus, the specific form of the loss function is

$$L(y_0) = 1 - q^{y_0} + \frac{Nq^{y_0}}{\langle x \rangle + N}. \quad (\text{B.9})$$

It is noteworthy that in the absence of the first stage, i.e. in the hypothesis of a pure geometric distribution, the value of L would be 1, not dependent on the value of y_0 . In this sense, the geometrical and the Poisson distributions are equivalent. The minimum value of L in Eq. B.9 as a function of y_0 is obtained for $y_0 = 0$, i.e. just after the end of the first stage, when the $N - 1$ upper cells of the system are full. And this minimum value is

$$L_{min} = \frac{N}{\langle n \rangle}. \quad (\text{B.10})$$

This result constitutes a rigorous lower bound for the expected accuracy of any forecasting strategy in the minimalist model. For this model, $\langle n \rangle$ increases rapidly as N grows (Gómez and Pacheco, 2004). This implies that the minimum L , obtained with this optimal forecasting strategy, decreases as N increases, as shown by the curve labeled as “Ideal” in Fig. 4.2. That is to say, minimalist models with more cells are more predictable.

References

- Aki, K., 1981. A probabilistic synthesis of precursory phenomena. In: Simpson, D.W., Richards, P.G. (Eds.), *Earthquake Prediction: An International Review*. American Geophysical Union, Washington D. C., Maurice Ewing Series, vol. 4, pp. 566-574.
- Aki, K., 1984. Asperities, barriers, characteristic earthquakes and strong motion prediction. *Journal of Geophysical Research* 89, 5867-5872.

- Bak, P., Tang, C., 1989. Earthquakes as a self-organized critical phenomenon. *Journal of Geophysical Research* 94, 15635-15637.
- Ben-Zion, Y., 2001. Dynamic ruptures in recent models of earthquake faults, *Journal of the Mechanics and Physics of Solids* 49, 2209-2244.
- Boness, N.L., Zoback, M.D., 2004. Stress-induced seismic velocity anisotropy and physical properties in the SAFOD Pilot Hole in Parkfield, CA. *Geophysical Research Letters* 31, L15S17, doi:10.1029/2003GL019020.
- Castellaro, S., Mulargia, F., 2001. A simple but effective cellular automaton for earthquakes. *Geophysical Journal International* 144, 609-624.
- Coppersmith, K.J., Schwartz, D.P., 1983. The characteristic earthquake model: Implications to recurrence on the San Andreas fault (abstract). *Earthquake Notes* 54, 61.
- Dahmen, K., Ertas, D., Ben-Zion, Y., 1998. Gutenberg-Richter and characteristic earthquake behavior in simple mean-field models of heterogeneous faults. *Physical Review E* 58, 1494-1501.
- Das, S., 2003. Spontaneous complex earthquake rupture propagation. *Pure and Applied Geophysics* 160, 579-602.
- Das, S., Aki, K., 1977. Fault plane with barriers: a versatile earthquake model. *Journal of Geophysical Research* 82, 5658-5670.
- Dowrick, D.J., Rhoades, D.A., 2004. Relations between earthquake magnitude and fault rupture dimensions: How regionally variable are they? *Bulletin of the Seismological Society of America* 94, 776-788.
- Drossel, B., Schwabl, F., 1992. Self-organized criticality in a forest-fire model. *Physica A* 191, 47-50.
- Fitzenz, D.D., Miller, S.A., 2004. New insights on stress rotations from a forward regional model of the San Andreas fault system near its Big Bend in southern California. *Journal of Geophysical Research* 109, B08404, doi:10.1029/2003JB002890.
- Frohlich, C., Davis, S.D., 1993. Teleseismic *b* values; or, much Ado about 1.0. *Journal of Geophysical Research* 98, 631-644.
- Gerstenberger, M.; Wiemer, S., Giardini, D., 2001. A systematic test of the hypothesis that the *b* value varies with depth in California. *Geophysical Research Letters* 28, 57-60.
- Goltz, C., 1997. *Fractal and Chaotic Properties of Earthquakes*. Springer-Verlag, Berlin, Germany, p. 178.
- Gómez, J.B., Pacheco, A.F., 2004. The minimalist model of characteristic earthquakes as a useful tool for description of the recurrence of large earthquakes. *Bulletin of the Seismological Society of America* 94, 1960-1967.
- González, Á., Gómez, J.B., Pacheco, A.F., 2005. The occupation of a box as a toy model for the seismic cycle of a fault. *American Journal of Physics*, in press. <http://arxiv.org/abs/physics/0502048>
- González, Á., Vázquez-Prada, M., Gómez, J.B., Pacheco, A.F., 2004. Using synchronization to improve the forecasting of large relaxations in a cellular-automaton model. *Europhysics Letters* 68, 611-617.
- Grant, L.B., Gould, M.M., 2004. Assimilation of paleoseismic data for earth-

- quake simulation. *Pure and Applied Geophysics* 161, 2295-2306.
- Gutenberg, B., Richter, C.F., 1944. Frequency of earthquakes in California. *Bulletin of the Seismological Society of America* 34, 185-188.
- Gutenberg, B. and Richter, C.F., 1954. *Seismicity of the Earth and Associated Phenomena*, 2nd edn. Princeton University Press, Princeton, New Jersey, USA, p. 310.
- Hainzl, S., Zöller, G., 2001. The role of disorder and stress concentration in nonconservative fault systems. *Physica A* 294, 67-84.
- Hainzl, S., Zöller, G., Kurths, J., 1999. Self-organized criticality model for earthquakes: Quiescence, foreshocks and aftershocks. *International Journal of Bifurcation and Chaos* 9, 2249-2255.
- Hainzl, S., Zöller, G., Kurths, J., Zschau, J., 2000. Seismic quiescence as an indicator for large earthquakes in a system of self-organized criticality. *Geophysical Research Letters* 27, 597-600.
- Harris, R.A., 2000. Earthquake stress triggers, stress shadows, and seismic hazard. *Current Science* 79, 1215-1225.
- Hashimoto, M., 2001. Complexity in the recurrence of large earthquakes in southwestern Japan: A simulation with an interacting fault system model. *Earth, Planets and Space* 53, 249-259.
- Heimpel, M.H., 2003. Characteristic scales of earthquake rupture from numerical models. *Nonlinear Processes in Geophysics* 10, 573-584.
- Helmstetter, A., Kagan, Y.Y., Jackson, D.D., 2005. Importance of small earthquakes for stress transfers and earthquake triggering. *Journal of Geophysical Research* 110, B05S08, doi:10.1029/2004JB003286.
- Henley, C.L., 1993. Statics of a “self-organized” percolation model. *Physical Review Letters* 71, 2741-2744.
- Hickman, S., Zoback, M., 2004. Stress orientations and magnitudes in the SAFOD pilot hole. *Geophysical Research Letters* 31, L15S12, doi:10.1029/2004GL020043.
- Houghton, J., 2002. *The Physics of Atmospheres*. Cambridge University Press, Cambridge, UK, p. 320.
- Ikeda, R., Iio, Y., Omura, K., 2001. In situ stress measurements in NIED boreholes in and around the fault zone near the 1995 Hyogo-ken Nanbu earthquake, Japan. *The Island Arc* 10, 252-260.
- Ishimoto, M., Iida, K., 1939. Observations sur les séismes enregistrés par le microséismographe construit dernièrement (I). *Bulletin of the Earthquake Research Institute, University of Tokyo* 17, 443-478.
- Kagan, Y.Y., 1996. Comment on “The Gutenberg-Richter or characteristic earthquake distribution, which is it?” by Steven G. Wesnousky. *Bulletin of the Seismological Society of America* 86, 274-285.
- Kagan, Y.Y., 1999. Universality of the seismic moment-frequency relation. *Pure and Applied Geophysics* 155, 537-573.
- Kanamori, H., Anderson, D.L., 1975. Theoretical basis of some empirical relations in seismology. *Bulletin of the Seismological Society of America* 65, 1073-1095.

- Kanamori, H., Brodsky, E.E., 2004. The physics of earthquakes. *Reports on Progress in Physics* 67, 1429-1496.
- Kanamori, H., Stewart, G.S., 1978. Seismological aspects of Guatemala earthquake on february 4, 1976. *Journal of Geophysical Research* 83, 3427-3434.
- Kato, N., Seno, T., 2003. Hypocenter depths of large interplate earthquakes and their relation to seismic coupling. *Earth and Planetary Science Letters* 210, 53-63.
- Keilis-Borok, V.I., 2002. Earthquake prediction: State-of-the-art and emerging possibilities. *Annual Review of Earth and Planetary Sciences* 30, 1-33.
- Keilis-Borok, V.I., Soloviev, A.A. (Eds.), 2003. *Nonlinear Dynamics of the Lithosphere and Earthquake Prediction*, Springer, Berlin, p. 337.
- Kisslinger, C., 1996. Aftershocks and fault-zone properties. *Advances in Geophysics* 38, 1-36.
- Kossobokov, V.G., Romashkova, L.L., Keilis-Borok, V.I., Healy, J.H., 1999. Testing earthquake prediction algorithms: Statistically significant advance prediction of the largest earthquakes in the Circum-Pacific, 1992-1997. *Physics of the Earth and Planetary Interiors* 111, 187-196.
- Kuroki, H., Ito, H.M., Takayama, H., Yoshida, A., 2004. 3-D simulation of the occurrence of slow slip events in the Tokai region with a rate- and state-dependent friction law. *Bulletin of the Seismological Society of America* 94, 2037-2050.
- Lei, X., Kusunose, K., Satoh, T., Nishizawa, O., 2003. The hierarchical rupture process of a fault: An experimental study. *Physics of the Earth and Planetary Interiors* 137, 213-228.
- López-Ruiz, R., Vázquez-Prada, M., Gómez, J.B., Pacheco, A.F., 2004. A model of characteristic earthquakes and its implications for regional seismicity. *Terra Nova* 16, 116-120.
- Main, I., 1996. Statistical physics, seismogenesis, and seismic hazard. *Reviews of Geophysics* 34, 433-462.
- Mason, I.B., 2003. Binary forecasts. In: Joliffe, I.T., Stephenson D.B (Eds.), *Forecast Verification: A Practitioners' Guide in Atmospheric Science*. Wiley, West Sussex, England, pp. 37-76 (references in pp. 215-226).
- Michael, A.J., 2005. Viscoelasticity, postseismic slip, fault interactions, and the recurrence of large earthquakes. *Bulletin of the Seismological Society of America*, in press.
- Miller, S.A., Ben-Zion, Y., Burg, J.-P., 1999. A three-dimensional fluid-controlled earthquake model: Behavior and implications. *Journal of Geophysical Research* 104, 10621-10638.
- Molchan, G.M., 1997. Earthquake prediction as a decision-making problem. *Pure and Applied Geophysics* 149, 233-247.
- Molchan, G.M., Kronrod, T., Panza, G.F., 1997. Multiscale seismicity model for seismic risk. *Bulletin of the Seismological Society of America* 87, 1220-1229.
- Moreno, Y., Gómez, J.B., Pacheco, A.F., 1999. Self organized criticality in a fiber-bundle-type model. *Physica A* 274, 400-409.

- Newman, W.I., Turcotte, D.L., 2002. A simple model for the earthquake cycle combining self-organized complexity with critical point behavior. *Nonlinear Processes in Geophysics* 9, 453-461.
- Okada, T., Matsuzawa, T., Hasegawa, A., 2003. Comparison of source areas of $M4.8 \pm 0.1$ repeating earthquakes off Kamaishi, NE Japan: are asperities persistent features? *Earth and Planetary Science Letters* 213, 361-374.
- Olami, Z., Feder, H.J.S., Christensen, K., 1992. Self-organized criticality in a continuous, nonconservative cellular automaton modeling earthquakes. *Physical Review Letters* 68, 1244-1247.
- Palmer, T.N., Shutts, G.J., Hagedorn, R., Doblas-Reyes, F.J., Jung, T., Leutbecher, M., 2005. Representing model uncertainty in weather and climate prediction. *Annual Review of Earth and Planetary Sciences* 33, 163-193.
- Pepke, S.L., Carlson, J.M., 1994. Predictability of self-organizing systems. *Physical Review E* 50, 236-242.
- Preston, E.F., Sá Martins, J.S., Rundle, J.B., Anghel, M., Klein, W., 2000. Models of earthquake faults with long-range stress transfer. *Computing in Science and Engineering* 2, 34-41.
- Reinecker, J., Heidbach, O., Tingay, M., Connolly, P., Müller, B., 2004. The 2004 release of the World Stress Map (available online at www.world-stress-map.org).
- Robinson, R., 2004. Potential earthquake triggering in a complex fault network: the northern South Island, New Zealand. *Geophysical Journal International* 159, 734-748.
- Robinson, R., Benites, R., 2001. Upgrading a synthetic seismicity model for more realistic fault ruptures. *Geophysical Research Letters* 28, 1843-1846.
- Rubin, A.M., 2002. Aftershocks of microearthquakes as probes of the mechanics of rupture. *Journal of Geophysical Research* 107, 2142, doi:10.1029/2001JB000496.
- Rundle, J.B., Klein, W., 1993. Scaling and critical phenomena in a cellular automaton slider-block model for earthquakes. *Journal of Statistical Physics* 72, 405-413.
- Rundle, J.B., Rundle, P.B., Donnellan, A., Fox, G., 2004. Gutenberg-Richter statistics in topologically realistic system-level earthquake stress-evolution simulations. *Earth, Planets and Space* 56, 761-771.
- Rundle, P.B., Rundle, J.B., Tiampo, K.F., Sa Martins, J.S., McGinnis, S., Klein, W., 2001. Nonlinear network dynamics on earthquake fault systems. *Physical Review Letters* 87, 148501.
- Rundle, J.B., Turcotte, D.L., Shcherbakov, R., Klein, W., Sammis, C., 2003. Statistical physics approach to understanding the multiscale dynamics of earthquake fault systems. *Reviews of Geophysics* 41, 1019, doi:10.1029/2003RG000135.
- Scholz, C.H., 2002. *The Mechanics of Earthquakes and Faulting*. 2nd edn. Cambridge University Press. Cambridge, United Kingdom. p. 496.
- Scholz, C.H., Gupta, A., 2000. Fault interactions and seismic hazard. *Journal of Geodynamics* 29, 459-467.

- Schorlemmer, D., Wiemer, S., 2005. Microseismicity data forecast rupture area. *Nature* 434, 1086.
- Schwartz, D.P., Coppersmith, K.J., 1984. Fault behavior and characteristic earthquakes: Examples from the Wasatch and San Andreas fault zones. *Journal of Geophysical Research* 89, 5681-5698.
- Schwartz, D.P., Coppersmith, K.J., Swan III, F.H., Somerville, P. and Savage, W.U., 1981. Characteristic earthquakes on intraplate normal faults (abstract). *Earthquake Notes* 52, 71.
- Seeber, L., Armbruster, J.G., 2000. Earthquakes as beacons of stress change. *Nature* 407, 69-72.
- Sieh, K., 1996. The repetition of large-earthquake ruptures. *Proceedings of the National Academy of Sciences of the United States of America* 93, 3764-3771.
- Soloviev, A., Ismail-Zadeh, A., 2003. Models of dynamics of block-and-fault systems. In: Keilis-Borok, V.I. and Soloviev, A.A. (Eds.), *Nonlinear Dynamics of the Lithosphere and Earthquake Prediction*. Springer, Berlin, Germany, pp. 71-139 references in pp. 311-332),
- Stacy, S.J., McCloskey, J., 1999. Heterogeneity and the earthquake magnitude-frequency distribution. *Geophysical Research Letters* 26, 899-902.
- Stein, S., Newman, A., 2004. Characteristic and uncharacteristic earthquakes as possible artifacts: applications to the New Madrid and Wabash seismic zones. *Seismological Research Letters* 75, 173-187.
- Stirling, M., Rhoades, D., Berryman, K., 2002. Comparison of earthquake scaling relations derived from data of the instrumental and preinstrumental era. *Bulletin of the Seismological Society of America* 92, 812-830.
- Stirling, M.W., Wesnousky, S.G., Shimazaki, K., 1996. Fault trace complexity, cumulative slip, and the shape of the magnitude-frequency distribution for strike-slip faults: A global survey. *Geophysical Journal International* 124, 833-868.
- Tsukahara, H., Ikeda, R., Yamamoto, K., 2001. In situ stress measurements in a borehole close to the Nojima Fault. *The Island Arc* 10, 261-265.
- Turcotte, D.L., 1997. *Fractals and Chaos in Geology and Geophysics*, 2nd edition Cambridge University Press, Cambridge, UK, p. 412.
- Vázquez-Prada, M., González, Á., Gómez, J.B., Pacheco, A.F., 2002. A minimalist model of characteristic earthquakes. *Nonlinear Processes in Geophysics* 9, 513-519.
- Vázquez-Prada, M., González, Á., Gómez, J.B., Pacheco, A.F., 2003. Forecasting characteristic earthquakes in a minimalist model. *Nonlinear Processes in Geophysics* 10, 565-571.
- Ward, S.N., 2000. San Francisco Bay area earthquake simulations: A step toward a standard physical earthquake model. *Bulletin of the Seismological Society of America* 90, 370-386.
- Wells, D.L., Coppersmith, K.J., 1994. New empirical relationships among magnitude, rupture length, rupture width, rupture area, and surface displace-

- ment. *Bulletin of the Seismological Society of America* 84, 974-1002.
- Wesnousky, S.G., 1994. The Gutenberg-Richter or characteristic earthquake distribution, which is it? *Bulletin of the Seismological Society of America* 84, 1940-1959.
- Wesnousky, S.G., 1996. Reply to Kagan's comment on "The Gutenberg-Richter or characteristic earthquake distribution, which is it?". *Bulletin of the Seismological Society of America* 86, 286-291.
- Wesnousky, S.G.; Scholz, C.H.; Shimazaki, K., Matsuda, T., 1983. Earthquake frequency distribution and the mechanics of faulting. *Journal of Geophysical Research* 88, 9331-9340.
- Wyss, M., Habermann, R.E., 1988. Precursory seismic quiescence. *Pure and Applied Geophysics* 126, 319-332.
- Yabuki, T., Matsuura, M., 1992. Geodetic data inversion using a bayesian information criterion for spatial-distribution of fault slip. *Geophysical Journal International* 109, 363-375.
- Yagi, Y., Kikuchi, M., Yoshida, S., Sagiya, T., 1999. Comparison of the coseismic rupture with the aftershock distribution in the Hyuga-nada earthquakes of 1996. *Geophysical Research Letters* 26, 3161-3164.
- Yamamoto, K., Yabe, Y., 2001. Stresses at sites close to the Nojima Fault measured from core samples. *The Island Arc* 10, 266-281.
- Yeats, R.S., Sieh, K., Allen, C.R., 1997. *The Geology of Earthquakes*. Oxford University Press, New York, USA, p. 568.
- Youngs, R.R., Coppersmith, K.J., 1985. Implications of fault slip rates and earthquake recurrence models to probabilistic seismic hazard estimates. *Bulletin of the Seismological Society of America* 75, 939-964.
- Zoback, M.L., 1992. 1st-order and 2nd-order patterns of stress in the lithosphere—The World Stress Map project. *Journal of Geophysical Research* 97, 11703-11728.
- Zöller, G., Holschneider, M., Ben-Zion, Y., 2005. The role of heterogeneities as a tuning parameter of earthquakes dynamics. *Pure and Applied Geophysics* 162, 1027-1049.